

## A Study on the Behavior of Combustion Wave Propagation and the Structure of Porous TiNi Body during Self-propagating High-temperature Synthesis Process

Ji Soon Kim\*, Victor E. Gjunter<sup>a</sup>, Jin Chun Kim, and Young Soon Kwon

*School of Materials Science and Engineering, University of Ulsan, Ulsan 680-749, Korea*

*<sup>a</sup>Research Institute of Shape Memory Medical Materials, Tomsk 634034, Russia*

(Received January 15, 2010; Revised February 1, 2010; Accepted February 5, 2010)

**Abstract** We produced cylindrical porous TiNi bodies by Self-propagating High-temperature Synthesis (SHS) process, varying the heating schedule prior to ignition of a loose preform compact made from (Ti+Ni) powder mixture. To investigate the effect of the heating schedule on the behaviour of combustion wave propagation and the structure of porous TiNi shape-memory alloy (SMA) body, change of temperature in the compact during SHS process was measured as a function of time and used for determining combustion temperature and combustion wave velocity. Microstructure of produced porous TiNi SMA body was observed and the results were discussed with the combustion characteristics. From the results it was concluded that the final average pore size could be controlled either by the combustion wave velocity or by the average temperature of the preform compact prior to ignition.

**Keywords** : TiNi porous body, Self-propagating high-temperature synthesis (SHS), Combustion wave propagation

### 1. Introduction

Titanium-nickel intermetallic compound is a representative shape memory alloy (SMA) with unique characteristics such as thermal shape memory effect, superelasticity, good corrosion resistance, and high damping properties. These properties can be used ideally for biomedical applications. In fact TiNi SMA implants have been developed and are widely used in cardiovascular and gastrointestinal applications [1-4]. As a biomaterial for hard-tissue replacement a porous TiNi SMAs are more suitable, because their stiffness and Young's modulus can be easily adjusted by controlling the porosity, and the porous structure would allow the in-growth of human tissue, nutrition exchange, and medicament transportation. In addition, porous alloys are lightweight. All these factors have made porous TiNi SMAs one of

the promising biomaterials for orthopedic implants and hard-tissue replacements [3-6].

A SHS (Self-Propagating High-temperature Synthesis) process is a very suitable for the production of porous TiNi shape memory alloy. The synthesis reaction occurs generally through ignition, propagation of a combustion wave front and cooling. It has advantages such as process economics, simplicity and purification of the reaction product [7-8]. Many of research works on the production of porous TiNi SMAs by SHS have been reported [9-11]. However, the studies on the relationship between the processing variable and the structure of porous TiNi SMAs are rarely found yet. Even in our previous works on the fabrication of porous TiNi SMAs by SHS process only a limited information had been simply given such as the effect of starting powder of Ti and Ni, the size of preform compact and the heating

---

\*Corresponding Author : [Tel : +82-52-259-2244; E-mail : jskim@ulsan.ac.kr]

schedule prior to the ignition on the pore size and the structure of TiNi SMAs produced [12-14]. In the present work we aimed at providing a basic experimental data which can be used for suggesting a possible relationship between the temperature change in the preform of (Ti+Ni) powder mixture, the combustion wave propagation behaviour and the structure of TiNi SMAs produced.

## 2. Experimental Procedures

Starting powders of Ti and Ni were mixed in an argon-gas sealed container using a ball mill to have a composition of Ti:Ni=50:50 at% and then vacuum-dried at 70°C. The prepared powder mixture was loaded in a quartz tube with diameters of 40 mm, and loose-compacted by tapping, where three thermocouples were inserted at 'top', 'centre' and 'bottom' position in a compact for measuring the temperature at various positions during the SHS process in real-time. For a synthesis reaction the compacted preform was loaded into a tube furnace under flowing argon-gas with a heating rate of 20 K/minute and ignited electrically with the use of a tungsten filament. For heating prior to ignition, three different heating schedules were used: (1) A-type (heated to 300°C and instantly ignited), (2) B-type (heated to 300°C, soaked for 1hour and then ignited), and (3) C-type (heated to 320°C followed by furnace-cooling to 300°C and then ignited). After the SHS reaction the compact was cooled to room temperature. During the SHS process temperature was measured real-time by three thermocouples in an analog signal which was converted automatically into digital data by microprocessor and stored in a computer. More detailed production procedure can be found in our previous papers [12-14]. The produced porous TiNi SMAs were cross-sectioned by electric-discharge wire-cutting after removing the surface layer which remained not reacted. Phase identification of the cross-section by X-ray diffractometry (XRD) showed a same result with our previ-

ous report: TiNi (B2) phase as a main phase with a trace of TiNi (B19') phase [13]. The structure of porous body was observed by optical and scanning electron microscopy (SEM), respectively. Image analysis program was used for analyzing the pore characteristics such as pore size and its distribution.

## 3. Results and Discussion

Fig. 1 shows a change in temperature profile during heating prior to ignition and during SHS reaction, respectively. As clearly seen in the Fig. 1(a), a temperature difference existed in a preform of (Ti+Ni) powder mixture during the process. Especially for the heating schedule of A-type, it was remarkable from position to position. The 'top' part showed the highest temperature and the 'center' part the lowest. For the heating schedule of B- and C-type the difference in temperature was not so large compared to the A-type. Such difference of temperature distribution seemed to be resulted from the different thermal conduction due to different positions in a preform and heating schedule. This temperature difference in a preform during a heating prior to ignition affected also the temperature change during combustion (Fig. 1(b)). The time at which the temperature increases after ignition was different according to the heating schedule and the position in a preform. This implies that a combustion wave would propagate in a different way depending on the heating schedule prior to ignition because the wave propagation behaviour has a close relationship with combustion temperature. A summary of measured temperatures in a preform compact at the moment of ignition and the temperature after combustion was given in In Fig. 2.

In A-type heating the 'centre' part showed lower temperature than 'top' and 'bottom' part, whereas B- and C-type revealed almost same temperature. Distribution of temperature in the preform seemed to be homogenized by the heating schedule of B- and C-type. From the results of the temperature after com-

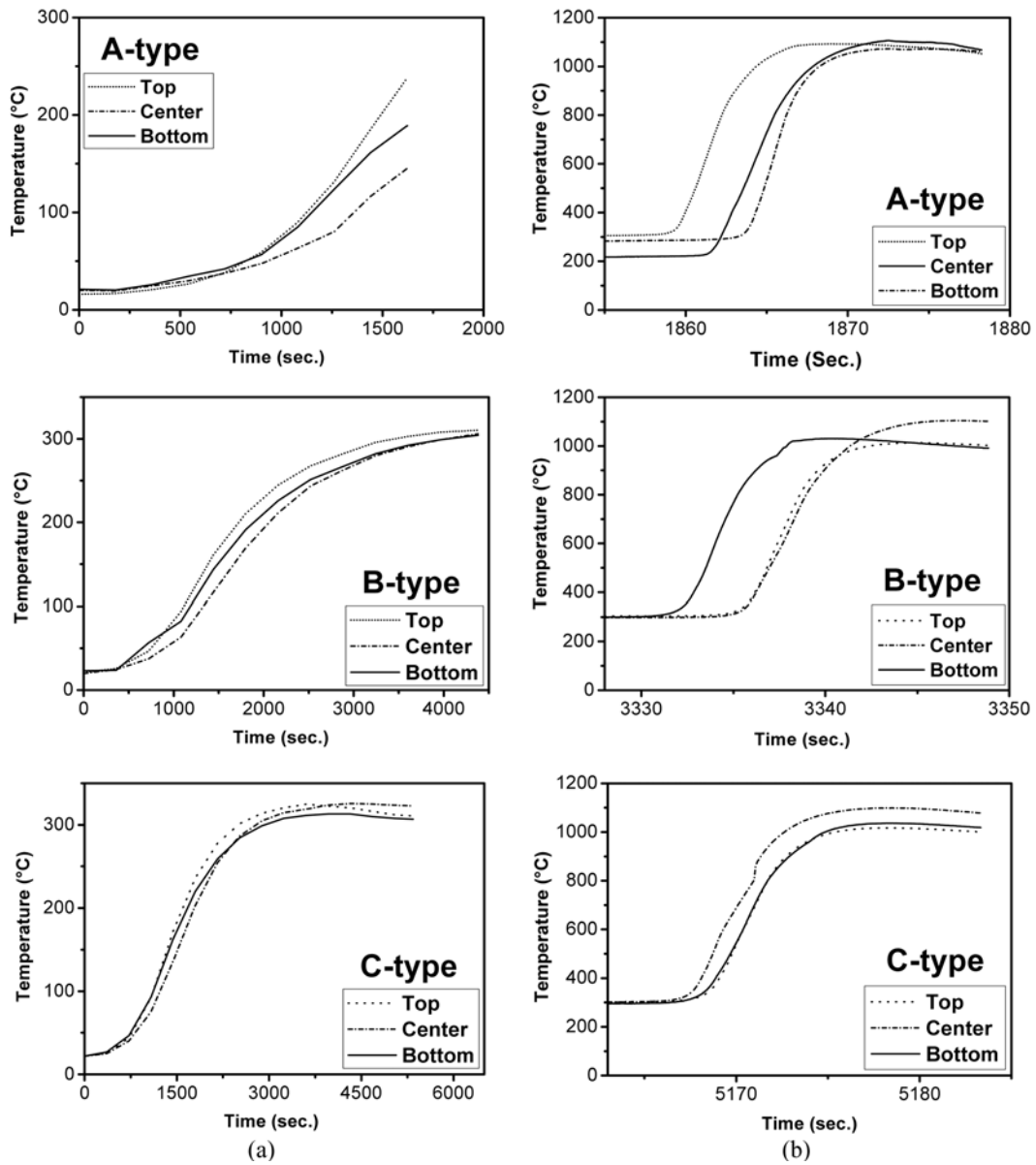


Fig. 1. Change in temperature (a) during heating prior to ignition and (b) during SHS reaction after ignition.

bustion we confirmed also a similar trend, that is, B- and C-type showed almost no difference with each other, but A-type showed a higher temperature both at 'top' and 'bottom' part. The maximum temperature after combustion was same as 1100°C at the 'centre' position for all the samples, irrespective of the heating schedule. It seems that the combustion behaviour might be affected by the temperature dis-

tribution in the preform prior to ignition.

Fig. 3 shows a change in the maximum temperature after combustion and the maximum combustion wave velocity as a function of average temperature in a preform compact at the moment of ignition. The data point was collected from all samples, irrespective of the heating schedule and the measured position, and averaged. In spite of scattering of data

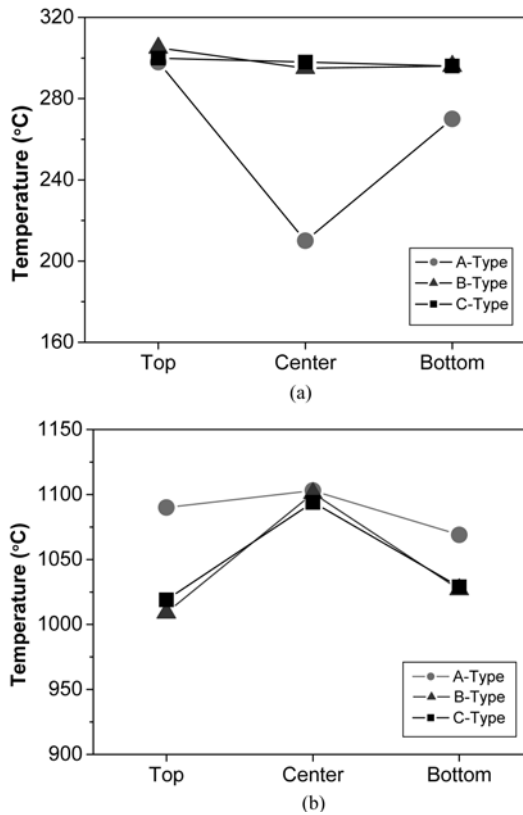


Fig. 2. (a) Temperature in a preform compact at the moment of ignition and (b) the maximum temperature after combustion.

points, it can be seen clearly that a relationship between the average temperature in a preform, the maximum temperature after combustion and the velocity of combustion wave exists. It is known that adiabatic combustion temperature of  $(\text{Ti}+\text{Ni} \rightarrow \text{TiNi})$  is normally higher than the melting point of TiNi ( $1310^\circ\text{C}$ ) [15] and can be further increased by pre-heating [16]. The data in Fig. 3 shows a different result. That is, the maximum temperature of combustion was lower than the reported one. A possible explanation can be given by the cooling effect of flowing argon gas and the porous structure of specimen. During the whole SHS process the furnace was protected under flowing argon gas and the flowing rate was drastically increased from the moment of ignition with intention. Additionally

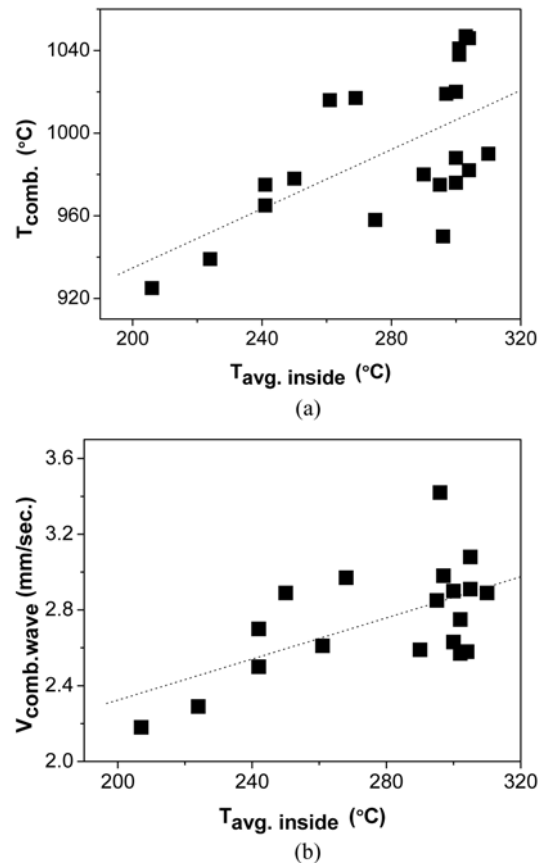


Fig. 3. Change in (a) the maximum temperature after combustion and (b) the maximum combustion wave velocity as a function of average temperature in a preform compact at the moment of ignition.

the open-channelled structure of specimen with high porosity seems to enhance the cooling effect further.

Another relationship between the maximum temperature after combustion and the combustion wave velocity could be also derived and given in Fig. 4. It seems that the combustion wave velocity increases exponentially with the maximum temperature after combustion, but it should be confirmed for a more clear explanation by further investigations.

To confirm the effect of the temperature difference in the preform on the combustion behaviour a similar graph as Fig. 3 was shown in Fig. 5, in this case, as a function of average temperature differ-

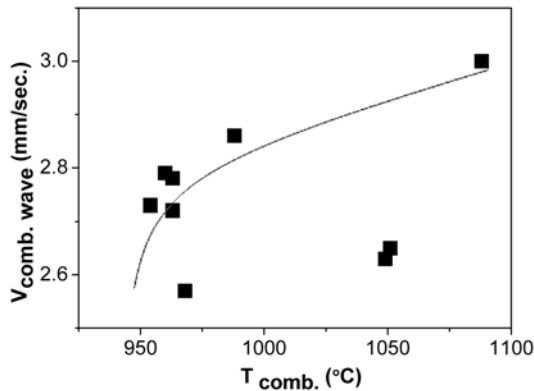


Fig. 4. Change in combustion wave velocity as a function of the maximum temperature after combustion.

ence between surface and inside of a preform compact at the moment of ignition. It is evident that an increase in temperature difference between the surface and inside a preform leads to an increase in the maximum temperature after combustion and the combustion wave velocity. It should be also noted here that the 'centre' part shows higher temperatures after combustion and lower combustion wave velocity compared to other parts.

Fig. 6 shows optical micrographs of the cross-section of porous TiNi SMAs produced and SEM images revealing a typical macro- and micro-pores inside the porous body. A wave pattern of concentric circle is found in the sample produced by the heating schedule A which represents an unstable propagation of combustion wave. The average pore size measured by image analysis method was in the range of 270-340 μm. All the samples had a three dimensionally interconnected open porous structure with TiNi SMA strut containing many closed pores with smaller size.

Fig. 7 shows a relationship between the pore size and the combustion characteristics like combustion temperature and combustion wave velocity, that is, change in pore size as a function of the maximum temperature after combustion, the combustion wave velocity and the average tempera-

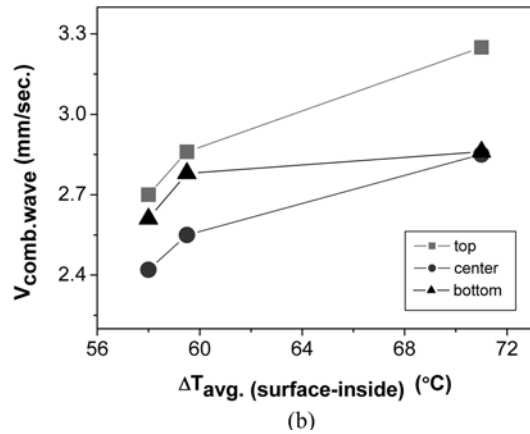
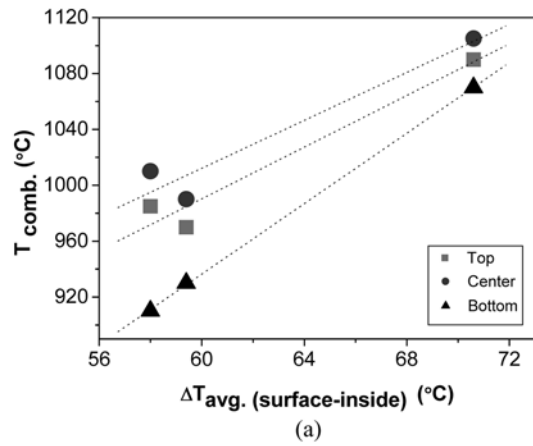


Fig. 5. Change in (a) the maximum temperature after combustion and (b) the maximum combustion wave velocity as a function of average temperature difference between surface and inside of a preform compact at the moment of ignition.

ture in a preform compact at the moment of ignition. It is difficult to find a relationship between the pore size and the maximum temperature after combustion. But it is clearly seen that the pore size has nearly a linear relationship with the combustion wave velocity and the average temperature in a preform prior to ignition. A linear relationship is more evident for the latter and it is more favourable from the point of view which can be more easily and usefully applied to the fabrication process for obtaining the porous TiNi SMAs with controlled pore size and structure.

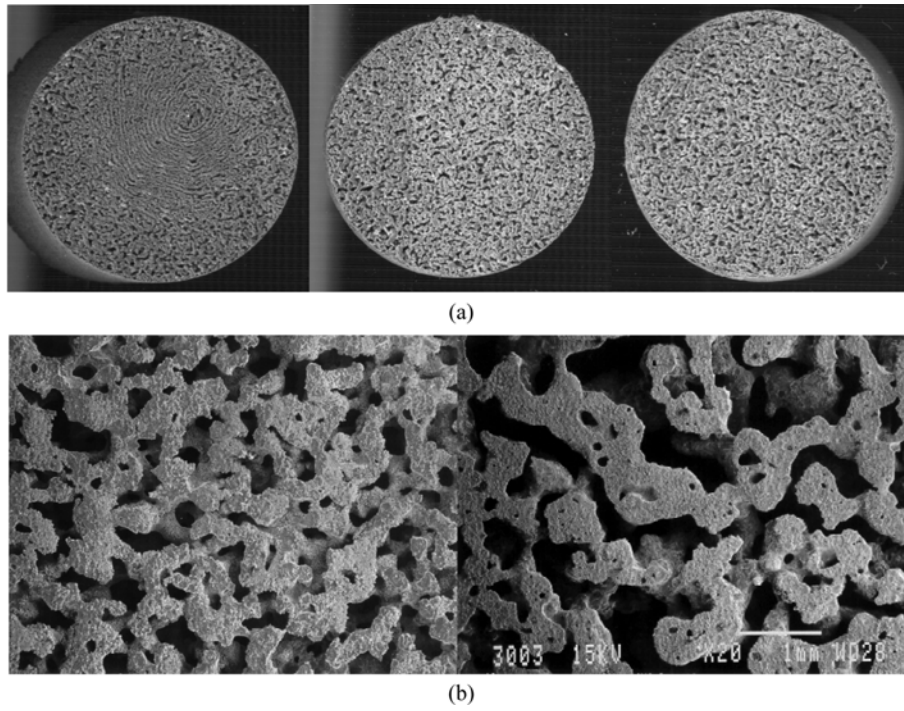


Fig. 6. (a) Optical micrographs of the cross-section of porous TiNi SMAs produced (from left A-, B- and C-type) (Diameter=40 mm) and (b) SEM images showing a typical macro- (left, x5) and micro-pores (right, x20) inside the porous body.

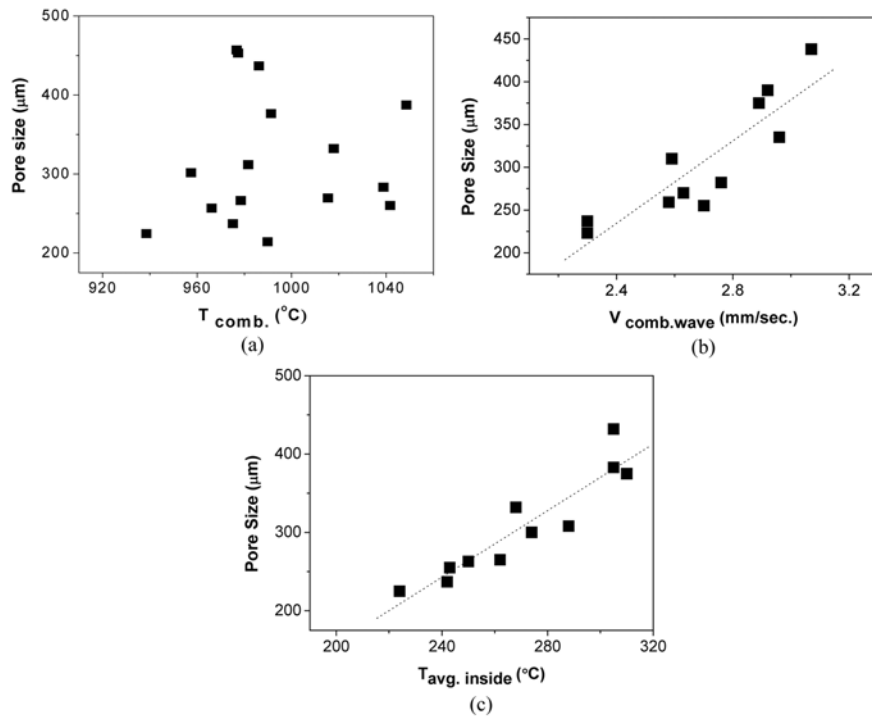


Fig. 7. Change in pore size as a function of (a) the maximum temperature after combustion, (b) the combustion wave velocity and (c) the average temperature in a preform compact at the moment of ignition.

#### 4. Conclusions

Porous TiNi SMAs were produced by SHS process. The difference in heating schedule prior to ignition of (Ti+Ni) loose powder preform led to different temperature distribution which was accompanied by a change in the combustion temperature and the propagation velocity of combustion wave during SHS process. Pore size increased with the propagation velocity and the average temperature inside the preform compact prior to ignition.

#### Acknowledgements

This work was supported by the 2007 Research Fund of the University of Ulsan.

#### References

- [1] K. Otsuka and C. M. Wayman: *Shape Memory Materials*, 1st ed., Cambridge University Press, Cambridge, United Kingdom, (1998) 220.
- [2] D. Y. Li: *Smart Mater. Struct.*, **9** (2000) 717.
- [3] J. A. Helsen and H. J. Breme: *Metals as Biomaterials*, 1st ed., John Wiley & Sons, Chichester, United Kingdom, (1998) 73.
- [4] A. Pelton, D. Hodgson and T. Duerig: *Proc. 1st Int. Conf. on Shape Memory and Superelastic Technologies, SMST-94, SMST Proc.*, Pacific Grove, CA, (1997) 449.
- [5] B. Silberstein: *Proc. Int. Conf. on Shape Memory and Superelastic Technologies (SMST-1997)*, Monterey, USA, (1997) 617.
- [6] L. H. Yahia: *Shape Memory Implants*, 1st ed., Springer, Berlin, (2000) 147.
- [7] A. G. Merzhanov, *Experimental Heat Transfer, Fluid Mechanics and Thermodynamics: Edizioni ETS, Pisa, Italy*, (1997) 1869.
- [8] J. J. Moore and H. J. Feng: *Progress in Materials Science*, **39** (1995) 243.
- [9] V. I. Itin, V. E. Gjunter, S. A. Shabalovskaya, and R. L. C. Sachdeva: *Mater. Characterization*, **32** (1994) 179.
- [10] C. L. Chu, B. Li, S. D. Wang, S. G. Zhang, X. X. Yang, and Z. D. Yin: *Trans. Nonferrous Met. Soc. China*, **7** (1997) 84.
- [11] B. Y. Li, L. J. Rong, Y. Y. Li and V. E. Gjunter: *J. Mater. Res.*, **15** (2000) 10.
- [12] J. S. Kim, S. H. Lee, J. H. Kang, V. E. Gjunter, S. B. Kang, T. H. Nam and Y. S. Kwon: *Proc. Int. Conf. on Shape Memory and Superelastic Technologies (SMST-2000)*, California, USA, (2000) 77.
- [13] J. S. Kim, J. H. Kang, S. B. Kang, K. S. Yoon and Y. S. Kwon: *Adv. Eng. Mater.*, **6** (2004) 403.
- [14] J. S. Kim, J. H. Song, M. G. Chang, Y. J. Yum, J. K. Lee and Y. S. Kwon: *J. Ceramic Proc. Res.*, **8** (2007) 70.
- [15] H. C. Yi and J. J. Moore: *Combustion and Plasma Synthesis of High-temperature Materials*, 1st ed., VCH Publishers, Inc., New York, (1990) 122.
- [16] J. B. Holt and Z. A. Munir: *J. Mater. Sci.*, **21** (1986) 251.